CrossMark

*J. Plasma Physics* (2015), *vol.* 81, 905810306 © Cambridge University Press 2015 
doi:10.1017/S002237781400124X

# Validating modeling assumptions of alpha particles in electrostatic turbulence

**G. J. Wilkie[1]†, I. G. Abel[2], E. G. Highcock[3] and W. Dorland[1]**

[1]University of Maryland, College Park, MD 20742, USA
[2]Princeton University, Princeton, NJ 08544, USA
[3]University of Oxford, Oxford OX1 3NP, UK

(Received 21 August 2014; revised 1 December 2014; accepted 1 December 2014;
first published online 21 January 2015)

To rigorously model fast ions in fusion plasmas, a non-Maxwellian equilibrium distribution must be used. In this work, the response of high-energy alpha particles to electrostatic turbulence has been analyzed for several different tokamak parameters. Our results are consistent with known scalings and experimental evidence that alpha particles are generally well confined: on the order of several seconds. It is also confirmed that the effect of alphas on the turbulence is negligible at realistically low concentrations, consistent with linear theory. It is demonstrated that the usual practice of using a high-temperature Maxwellian, while previously shown to give an adequate order-of-magnitude estimate of the diffusion coefficient, gives incorrect estimates for the radial alpha particle flux, and a method of correcting it in general is provided. Furthermore, we see that the timescales associated with collisions and transport compete at moderate energies, calling into question the assumption that alpha particles remain confined to a flux surface that is used in the derivation of the slowing-down distribution.

## 1. Introduction

The study of fusion-related plasmas is intimately concerned with the behavior of alpha particles, which initially carry an energy of $E_\alpha \equiv 3.5$ MeV as a product of the deuterium–tritium (DT) nuclear fusion reaction, which is much faster than the $\sim$10 keV ions that make up the plasma bulk. The high-energy alpha particles give up their energy by colliding against cooler bulk ions and electrons, eventually forming a high-energy tail in collisional equilibrium (see Gaffey 1976).

How well this non-Maxwellian population of high-energy particles is confined is therefore a critical question for the possibility of achieving ignition. Although electrons absorb most of the collisional heating from the energetic particles, the remaining 30–40% of the energy that gets transferred to the ions (Stix 1973) will be an important heating mechanism in future fusion devices. It is then no surprise that there has been a considerable amount of work done on the topic. Estrada-Mila et al. (2006) performed numerical simulations using `GYRO` (Candy and Waltz 2003) and found significant transport of high-energy alpha particles in the core due to electrostatic turbulence. This was confirmed by Albergante et al. (2009) using `GENE` (Jenko et al. 2000), and it was stressed that turbulence can result in the retention of low-energy helium ash, a result which Angioni et al. (2009) also found with `GS2` (Kotschenreuther

† Email address for correspondence: gwilkie@umd.edu

https://doi.org/10.1017/S002237781400124X Published online by Cambridge University Press

et al. 1995; Dorland et al. 2000). All of these nonlinear gyrokinetic simulations of alpha particle transport were performed by treating the alpha particle population as a hot Maxwellian species, using the so-called 'equivalent Maxwellian' approximation. This approximation has been in use for a long time (e.g. Rosenbluth and Rutherford 1975), and was formalized by Estrada-Mila et al. (2006).

However, alpha particles are not Maxwellian in reality (Gaffey 1976), a fact which is well recognized in the above references. Indeed, care was taken to show that using a Maxwellian of the same temperature gave accurate linear results. Then, quasilinear simulations in GS2 were performed using the non-Maxwellian slowing-down distribution (Angioni and Peeters 2008) to obtain the radial flux of alpha particles, where attention was drawn to the incorrectness of the radial gradient of the equivalent Maxwellian. In this work, we demonstrate that the numerical value of the alpha particle flux can be poorly estimated, depending on the local parameters used. It was previously found that rough estimates (within about 50%) for the diffusion coefficient can be obtained using the Maxwellian approximation (Angioni and Peeters 2008), and we do not contradict this result. Even in cases where the equivalent Maxwellian is inadequate, we present a method to rigorously obtain the correct energy-dependent flux valid in the trace limit.

By treating the electrostatic ion-scale turbulence as a given background field with known properties, to which the energetic particles passively react, analytic scalings can be obtained. It was found (Estrada-Mila et al. 2006; Hauff et al. 2009) that the diffusion of energetic particles scales inversely with energy ($E^{-1}$) for particles with high pitch angle ($v_\parallel \sim v$), and as $E^{-3/2}$ for deeply-trapped energetic particles. It was later pointed out (Pueschel et al. 2012) that this is an expansion in Larmor radius, with the former result valid only for prohibitively large pitch angles for high-energy particles. Therefore, an overall $E^{-3/2}$ scaling is expected: a result we confirm.

In this work, we present a fully nonlinear self-consistent treatment of non-Maxwellian energetic particles. We use this capability to test commonly-made assumptions in the modeling of alpha particles in the context of turbulence. After reviewing our approach to the problem in Sec. 2, we will find in Sec. 3 that the passive-tracer limit is largely satisfactory. However, the equivalent-Maxwellian approach is not adequate in determining the transport properties of alpha particles (see Sec. 4). Later, in Sec. 5, we estimate how well alpha particles of various energies are confined for realistic equilibrium parameters, followed by a general discussion of these results.

## 2. Background: gyrokinetics of fast ions

Here we give a brief exposition of gyrokinetics with an eye to non-Maxwellian energetic particles. Usually, iterative expansions of gyrokinetics assumes that the collision frequency is much larger than the source/sink rate or the transport time, but we will relax that assumption here. The full derivation of the gyrokinetic ordering for weakly collisional species will be given in Abel and Schekochihin. We will assume here that the equilibrium distribution function is still isotropic in velocity space: that is, only a function of energy.

### 2.1. *Low-collisionality gyrokinetics*

Gyrokinetics is the standard tool for studying low-frequency, small-scale turbulence in highly magnetized plasmas. A strong magnetic field allows one to take advantage of the strong anisotropization of the dynamics that results, and one can perform an asymptotic expansion of the Fokker–Planck equation in the small parameter

https://doi.org/10.1017/S002237781400124X Published online by Cambridge University Press

$\rho^* \equiv \rho_i/a$, where $a$ is the minor radius of the device (representing the equilibrium scale length), $\rho_i = v_{ti}/\Omega_i$ is the characteristic Larmor radius of the bulk ions (with $v_{ts} \equiv \sqrt{2T_s/m_s}$ the thermal speed of species $s$ with temperature $T_s$ and mass $m_s$), and the gyrofrequency is $\Omega_s = Z_s eB/m_s c$. The equilibrium magnetic field $\mathbf{B}$, temperatures $T_s$, and densities $n_s$ vary on the scale of $a$, as do any fluctuating quantities along the magnetic field, characterized by the parallel wavenumber $k_\parallel$. The advantage of this expansion is that it allows an averaging over the fast gyro-motion while retaining fine-spatial-scale dynamics perpendicular to the field, characterized by the wavenumber $k_\perp$, the scale of which is allowed to be smaller than the Larmor radius. To summarize, the gyrokinetic ordering is such that

$$\frac{|\mathbf{v}_\mathbf{E}|}{v_{ti}} \sim \frac{k_\parallel}{k_\perp} \sim \frac{\omega}{\Omega_i} \sim \frac{\rho_i}{a} \equiv \rho^*, \tag{2.1}$$

where $\omega$ is a characteristic frequency associated with turbulent fluctuations in the distribution function, and $\mathbf{v}_\mathbf{E}$ is the $E \times B$ drift velocity. Contrast this with, for example, drift-kinetics or magnetohydrodynamics, which allow $v_E \sim v_{ti}$ or $\omega \sim \Omega_i$ respectively, but neither can resolve fluctuations with sizes comparable to a Larmor radius.

The distribution function is decomposed as

$$f_s\left(\mathbf{r}, E, \mu, \xi, \sigma_\parallel, t\right) = F_{0s} + \delta f_s = F_{0s} + Z_s e\phi \frac{\partial F_{0s}}{\partial E} + h_s, \tag{2.2}$$

and in general depends on spatial position $\mathbf{r}$ through the electrostatic potential $\phi(\mathbf{r}, t)$. In these coordinates, the sign of $v_\parallel$ must be specified by $\sigma_\parallel$ so that $v_\parallel = \sigma_\parallel \sqrt{(2/m_s)(E - \mu B)}$ and $v_\perp = \sqrt{2\mu B/m_s}$. The direction of $\mathbf{v}_\perp$ is determined from the gyro-phase $\xi$. The gyro-center position $\mathbf{R}_s$ is related to $\mathbf{r}$ by $\mathbf{r} = \mathbf{R}_s + \mathbf{b} \times \mathbf{v}_\perp/\Omega_s$. The slowly-evolving equilibrium distribution is $F_{0s}$, and is written this way when no particular velocity dependence is specified. We will introduce notations such as $F_{Ms}$ and $F_{Ss}$ later, and these shall be interpreted as specific forms of $F_{0s}$ with given velocity dependence. The non-adiabatic part of the perturbed distribution, $h_s \sim \rho^* F_{0s}$ is a function of gyro-center position and velocity, but does not depend on gyro-phase $\xi$. It is found by solving the gyrokinetic equation, which in the electrostatic ($\beta \to 0$) limit without equilibrium flow reads:

$$\begin{aligned} &\frac{\partial h_s}{\partial t} + \left(v_\parallel \mathbf{b} + \mathbf{v}_{\mathbf{d}s} \frac{c}{B} \mathbf{b} \times \nabla \langle\phi\rangle_{\mathbf{R}_s}\right) \cdot \nabla h_s - C_{GK}\left[h_s\right] - Z_s e \frac{\partial \langle\phi\rangle_{\mathbf{R}_s}}{\partial t} \frac{\partial h_s}{\partial E} \\ &\quad = -Z_s e \frac{\partial F_{0s}}{\partial E} \frac{\partial \langle\phi\rangle_{\mathbf{R}_s}}{\partial t} - \frac{c}{B} \mathbf{b} \times \nabla \langle\phi\rangle_{\mathbf{R}_s} \cdot \nabla F_{0s}, \end{aligned} \tag{2.3}$$

where $C_{GK}$ is an appropriate gyro-averaged collision operator (see Abel et al. 2008; Barnes et al. 2009; Li and Ernst 2011), $Z_s e$ is the charge carried by species $s$, and $\mathbf{v}_{\mathbf{d}s}$ is the velocity of magnetic drifts due to the curvature and gradient of $\mathbf{B}$. All gradients in (2.3) are with respect to the gyrocenter coordinate $\mathbf{R}_s$.

Equation (2.3) is closed by solving for the electrostatic potential via the quasineutrality condition:

$$\phi \sum_s Z_s^2 e^2 \int \frac{\partial F_{0s}}{\partial E} d^3\mathbf{v} + \sum_s Z_s e \int \langle h_s \rangle_\mathbf{r} \, d^3\mathbf{v} = 0, \tag{2.4}$$

in which $\langle\rangle_\mathbf{r}$ is the gyro-average operation at constant spatial position $\mathbf{r}$.

The form of (2.3) is identical to other iterative derivations of the gyrokinetic equation (see Frieman and Chen 1982; Sugama and Horton 1998; Abel et al. 2013),

https://doi.org/10.1017/S002237781400124X Published online by Cambridge University Press

except for the final term on the left-hand side. This is the so-called parallel nonlinearity as expressed in $E$, $\mu$ coordinates (its name comes from the form it takes in $v_\parallel$, $\mu$ coordinates). Its presence at this order is a consequence of the low-collisionality ordering because now, much finer velocity-space structures can develop in $h_\alpha$ such that $\partial h_\alpha/\partial E \sim (\rho^*)^{-1} h_\alpha/E$. Hamiltonian derivations of the gyrokinetic equation (Brizard and Hahm 2007) also include this nonlinearity, but for different reasons (e.g. its convenient conservation properties, see the appendix of Abel et al. (2013)). In order to properly resolve this term, one needs a velocity-space grid ($1/\rho^*$) finer than usual, making its inclusion numerically challenging. It is important to note that this term is only included in the gyrokinetic equation for the alpha particles; the distribution functions, $h_s$, for the bulk (non-energetic) species are obtained by solving the standard gyrokinetic equation with $F_{0s}$ Maxwellian.

At higher order in $\rho^*$, one obtains the transport equation, which now contains the collision operator acting on $F_{0s}$. After integrating over $\mu$ and summing over the sign of the parallel velocity, but preserving the energy dependence, the transport equation becomes:

$$\frac{1}{V'}\frac{\partial}{\partial t}V' F_{0s} + \frac{1}{V'}\frac{\partial}{\partial \psi}V' \Gamma_s(E) + \frac{1}{\sqrt{E}}\frac{\partial}{\partial E}\sqrt{E}\Gamma_{E,s}(E) = \langle C\left[F_{0s}\right] + S_s\rangle_\psi . \tag{2.5}$$

The source of particles of species $s$ is denoted as $S_s$. Equation (2.5) determines the slow-time evolution of the equilibrium, including the average transport of particles in phase space due to turbulence. The radial flux is:

$$\Gamma_s(E) \equiv \left\langle \sum_{\sigma_\parallel} \int h_s \langle \mathbf{v_E}\rangle_{\mathbf{R}_s} \cdot \nabla\psi \frac{\pi B \mathrm{d}\lambda}{\sqrt{1-\lambda B}} \right\rangle_{t,\psi}, \tag{2.6}$$

and the flux in energy, representing the acceleration of particles by fluctuations, is:

$$\Gamma_{E,s}(E) \equiv Z_s e \left\langle \sum_{\sigma_\parallel} \int h_s \frac{\partial \langle \phi\rangle_{\mathbf{R}_s}}{\partial t} \frac{\pi B \mathrm{d}\lambda}{\sqrt{1-\lambda B}} \right\rangle_{t,\psi}. \tag{2.7}$$

In these expressions, the coordinate $\lambda \equiv \mu/E$ is used here for convenience so that the velocity space volume element is separable. Also,

$$V'(\psi) \equiv \lim_{\delta\psi\to 0} \frac{1}{\delta\psi} \int_\Delta d^3\mathbf{r}, \tag{2.8}$$

where the domain of spatial integration $\Delta$ is the toroidal annulus formed between flux surfaces $\psi$ and $\psi + \delta\psi$. The average in the definition of the fluxes is the composition of the average $\langle \ldots\rangle_\psi$ over a flux tube at the radial location $\psi$ and the time average $\langle \ldots\rangle_t \equiv \frac{1}{T}\int_{t_0}^{t_0+T} \ldots dt$ over a time $T$. The width of the flux tube is taken to be several turbulent correlation lengths and the time $T$ to be many turbulent correlation times.

We define the energy-integrated particle and heat fluxes of species $s$ as follows:

$$\Gamma_s = \frac{\sqrt{2}}{m_s^{3/2}} \int \Gamma_s(E)\sqrt{E} dE, \tag{2.9}$$

and

$$Q_s = \frac{\sqrt{2}}{m_s^{3/2}} \int \Gamma_s(E) E^{3/2} dE. \tag{2.10}$$

https://doi.org/10.1017/S002237781400124X Published online by Cambridge University Press

Now, if we were to integrate (2.5) multiplied by powers of $E$ over all energies we would recover the usual transport equations for density and heat with fluxes defined by (2.9) and (2.10), respectively. Equation (2.6) defines the flux of particles that possess kinetic energy between $E$ and $E + \mathrm{d}E$ passing through a flux surface labeled by $\psi$. Using this definition means that if the distribution were an isotropic 'beam' of particles with energy $E_b = m_s v_b^2/2$ (i.e. $\delta f \propto \delta(E - E_b)$), then $\Gamma_\alpha(E) = \Gamma_\alpha \delta^3(\mathbf{v} - \mathbf{v_b})$. That is, $\Gamma(E)$ represents what the particle flux would be for a beam of energy $E$. To clarify the notation: $\Gamma_\alpha(E)$, defined in (2.7) is a different quantity than $\Gamma_\alpha$ (without explicit energy dependence), which is the integrated particle flux defined in (2.9).

If the collision operator is dominant in (2.5), we find that the solution is $F_{0s} = F_{Ms}$, the Maxwellian distribution:

$$F_{Ms} \equiv n_s \left(\frac{m_s}{2\pi T_s}\right)^{3/2} \exp\left(-\frac{m_s v^2}{2T_s}\right), \tag{2.11}$$

and terms such as $\partial F_{0s}/\partial E$ in (2.3) and (2.4) become $-F_{Ms}/T_s$. Knowing the form of $F_{0s}$, tools such as `Trinity` (Barnes et al. 2009) or `TGYRO` (Candy et al. 2009) solve for the moments of (2.5) (without the collision operator) to simulate the long-time global evolution of the toroidal device.

As our low-collisionality ordering permits an arbitrary $F_{0\alpha}(\psi, E)$, one loses the easily parametrized form of $F_{0\alpha}$. Thus, picking an $F_{0\alpha}$ necessitates guessing (or, finding experimentally or numerically) a solution to the transport equation (2.5). So, as a first step, let us employ further assumptions that allow us to use a known analytic form of $F_{0\alpha}$.

### 2.2. *Subsidiary expansion in $\tau_s/\tau_E$ for alphas*

To remedy the aforementioned complications associated with the low-collisionality ordering, for alpha particles we perform a subsidiary expansion on (2.3) and (2.5). Define a parameter $\delta \equiv \tau_s/\tau_E$ (not to be confused with the Dirac delta function, which always has an argument), where $\tau_E$ is the energy confinement time of the plasma bulk, representing the transport time scale, and $\tau_s$ is the slowing-down time, from the dominant collision frequency for high-energy alpha particles slowing down via drag on electrons (Helander and Sigmar 2002):

$$\tau_s \equiv \frac{3}{16\sqrt{\pi}} \frac{m_\alpha m_e v_{te}^3}{Z_\alpha^2 e^4 n_e \ln \Lambda}, \tag{2.12}$$

where $\ln \Lambda$ is the Coulomb logarithm. If we take $\delta \ll 1$, collisions are now a bit stronger so that the energy derivative is $\partial h_\alpha/\partial E \sim \mathrm{O}\left[\sqrt{\delta/\rho^*}\,(h_\alpha/E)\right]$, which results in a term we take to be small enough to leave out of the gyrokinetic equation. Now we have:

$$\begin{aligned} \frac{\partial h_s}{\partial t} + \left(v_\parallel \mathbf{b} + \mathbf{v}_{\mathbf{d}s}\frac{c}{B}\mathbf{b}\times\nabla\langle\phi\rangle_{\mathbf{R}_s}\right)\cdot\nabla h_s - C_{GK}[h_s] \\ = -Z_s e \frac{\partial F_{0s}}{\partial E}\frac{\partial \langle\phi\rangle_{\mathbf{R}_s}}{\partial t} - \frac{c}{B}\mathbf{b}\times\nabla\langle\phi\rangle_{\mathbf{R}_s}\cdot\nabla F_{0s}, \end{aligned} \tag{2.13}$$

and (2.5) becomes:

$$\frac{\partial F_{0s}}{\partial t} = C[F_{0s}] + \frac{\sigma}{4\pi v_\alpha^2}\delta(v - v_\alpha), \tag{2.14}$$

where $\sigma$ is the creation rate of alpha particles from fusion per unit volume per unit time. The alpha particle source is approximated here by a Dirac delta function at

https://doi.org/10.1017/S002237781400124X Published online by Cambridge University Press

| | | TFTR | JET | ITER |
|---|---|---|---|---|
| Toroidal ion gyroradius | $\rho_i/a$ | 0.0028 | 0.0037 | 0.0013 |
| Toroidal alpha gyroradius | $\rho_\alpha/a$ | 0.040 | 0.058 | 0.018 |
| Poloidal ion gyroradius | $\rho_{i,pol}/a$ | 0.026 | 0.026 | 0.0079 |
| Poloidal alpha gyroradius | $\rho_{\alpha,pol}/a$ | 0.37 | 0.41 | 0.11 |
| Ion–ion collision frequency | $\nu_{ii}a/v_{ti}$ | $2.7 \times 10^{-5}$ | $5.0 \times 10^{-5}$ | $1.6 \times 10^{-4}$ |
| $\alpha$-e slowing-down frequency | $\nu_s^{\alpha e}a/v_{ti}$ | $1.3 \times 10^{-6}$ | $2.4 \times 10^{-6}$ | $5.9 \times 10^{-6}$ |
| Slowing-down time (s) | $\tau_s$ | 0.48 | 1.0 | 0.85 |
| Energy confinement time (s) | $\tau_E$ | 0.13 | 0.59 | 2.98 |

TABLE 1. Properties of some typical tokamak properties, using the radial-average values from Budny (2002). Ion species is deuterium, and alpha particle parameters are taken at 3.5 MeV.

$v_\alpha = \sqrt{2E_\alpha/m_\alpha}$. The transport terms in (2.5) are smaller by a factor of $\delta$ and therefore do not appear in (2.14), consistent with our ordering.

Table 1 lists some characteristic parameters in several fusion devices. From inspection, one can see that the low-collisionality ordering is required, and the subsidiary expansion in $\tau_s/\tau_E$ is marginally justified, but only for ITER. In this work, we will use the turbulent flux of alpha particles to verify this expansion and that $\tau_\Gamma \sim \tau_E$, where the former is the alpha particle transport time, which is the relevant time scale for alpha particle transport in (2.5).

The reader may be justifiably concerned that the requirement that $\rho_s \ll a$ may be called into question for fast alpha particles due to their large Larmor orbits compared to the bulk ions. The Larmor radii of alpha particles is compared to the sizes of several large tokamaks in Table 1, where it can be seen that this approximation is in fact valid, even for newborn alphas at 3.5 MeV. A separate concern is the so-called banana-width created by the drift orbits of alpha particles due to gradients in the equilibrium magnetic field. The size of this orbit can be estimated by the poloidal Larmor radius: the Larmor radius using the poloidal magnetic field $\rho_{\alpha,pol} \equiv Z_\alpha e\mathbf{B}\cdot\mathbf{e}_\theta/m_\alpha c$. This is in fact large, and can cause significant loss of alphas if the orbit extends to the wall of the tokamak. Such loss mechanisms are important, but beyond the scope of this work; we restrict ourselves to studying the turbulence-induced electrostatic transport of otherwise well-confined alpha particles. For similar reasons, we will also assume that equilibrium properties do not vary significantly over an alpha particle drift orbit, which for ITER is about one tenth of the minor radius for the most energetic alpha particles. This last assumption allows us to use the flux-tube approximation.

### 2.3. *The slowing-down distribution*

The analytic 'slowing-down distribution' is the steady-state solution to an equation approximate to (2.14) that balances the collision operator with a fast particle source. If we set $\partial F_{0s}/\partial t = 0$ and approximate the collision operator in the range where $v_{ti} \ll v \ll v_{te}$, we can obtain the slowing-down distribution (see Gaffey 1976; Helander and Sigmar 2002):

$$F_{S\alpha}(v) = \frac{3}{4\pi \ln\left(1 + v_c^3/v_\alpha^3\right)} \frac{n_\alpha}{v_c^3 + v^3} H(v_\alpha - v), \tag{2.15}$$

https://doi.org/10.1017/S002237781400124X Published online by Cambridge University Press

where $H$ is the Heaviside step function, $n_\alpha$ is the equilibrium density of alpha particles, and

$$v_c \equiv v_{te}\left(\frac{3\sqrt{\pi}}{4}\sum_i \frac{n_i m_e}{n_e m_i} Z_i^2\right)^{1/3} \tag{2.16}$$

is the critical speed. Above this speed, alpha particles primarily lose their energy via drag on faster electrons, whereas below, they primarily drag against approximately stationary ions. It is important to note that (2.15) is only valid when $v \gg v_{ti}$. In fact, (2.14) lacks a steady state solution entirely, due to the particle source. The fact that (2.15) is a valid steady state for $v \gg v_{ti}$ suggests that the increasing alpha particle density must be manifest where $v \sim v_{ti}$. This is the buildup of helium ash in local thermal equilibrium with the main ions. This cold, Maxwellian helium is known to get periodically ejected by the plasma during sawtooth crashes (Nave et al. 2003).

In this work, we will not concern ourselves with the fate of the ash; we limit ourselves to the effects of and on the high-energy ($v \gg v_{ti}$) non-Maxwellian tail described by (2.15). We will find that the transport properties of alpha particles depend strongly on energy, so we must be careful not to extend our conclusions to regimes in which our distribution is not valid, namely $v \sim v_{ti}$. Unless otherwise stated, the term 'alpha particles' will refer to a non-Maxwellian species described by this slowing-down distribution.

To solve the gyrokinetic equation, we also need $\nabla F_{S\alpha}$ as a function of velocity. To obtain this, we apply the chain rule to (2.15), using the definition of $v_c$ in (2.16):

$$\begin{aligned}\frac{\nabla F_{S\alpha}}{F_{S\alpha}} &= \frac{1}{F_{S\alpha}}\frac{\partial F_{S\alpha}}{\partial n_\alpha}\nabla n_\alpha + \frac{1}{F_{S\alpha}}\frac{\partial F_{S\alpha}}{\partial v_c}\nabla v_c \\ &= \frac{\nabla n_\alpha}{n_\alpha} + \frac{1}{F_{S\alpha}}\frac{\partial F_{S\alpha}}{\partial v_c}\left(\frac{\partial v_c}{\partial T_e}\nabla T_e + \frac{\partial v_c}{\partial n_i}\nabla n_i + \frac{\partial v_c}{\partial n_e}\nabla n_e\right) \\ &= \frac{\nabla n_\alpha}{n_\alpha} + \left[\frac{v_\alpha^3}{v_c^3+v_\alpha^3}\frac{1}{\ln\left(1+v_\alpha^3/v_c^3\right)} - \frac{v_c^3}{v_c^3+v^3}\right] \\ &\quad\times\left(\frac{3}{2}\frac{\nabla T_e}{T_e} - \frac{\nabla n_e}{n_e} + \frac{\sum_i Z_i^2 \nabla n_i/m_i}{\sum_i Z_i^2 n_i/m_i}\right).\end{aligned} \tag{2.17}$$

Choose a suitable radial coordinate $\rho$ such that $\nabla F_{0s} = \nabla\rho\,\partial F_{0s}/\partial\rho$ (in our simulations it is defined as the half-diameter of the flux surface at the height of the magnetic axis). It will be convenient to define the gradient length scale of $v_c$ thusly:

$$\frac{1}{L_{v_c}} \equiv \frac{\partial}{\partial\rho}\ln v_c = \frac{3}{2}\frac{1}{L_{T_e}} - \frac{1}{L_{n_e}} + \frac{\sum_i Z_i^2 n_i/m_i L_{n_i}}{\sum_i Z_i^2 n_i/m_i}. \tag{2.18}$$

In the flux-tube approximation, we assume that this quantity, and others defined similarly for $T_i$, $n_e$, etc., are constant across the simulation domain.

In this section, we have briefly discussed the gyrokinetic framework and how it is modified when species are allowed to be non-Maxwellian. In order to solve the gyrokinetic (2.13) and associated field (2.4) equations, it will be necessary to keep $\partial F_{0s}/\partial E$ and $\nabla F_{0s}$ as more general functions of energy. This has been done with the `GS2` local flux-tube code, and in the following sections, we use this tool to test various assumptions made about alpha particles with self-consistent simulations.

https://doi.org/10.1017/S002237781400124X Published online by Cambridge University Press

### 2.4. *Simulation setup*

GS2 is a local flux-tube code that solves the gyrokinetic equation in field-following 'twist-and-shift' coordinates (Cowley et al. 1991), and is capable of handling arbitrary equilibrium $F_{0s}$. The 'cyclone base case' (Dimits et al. 2000) is characterized by an $\hat{s} - \alpha$ geometry with an aspect ratio of $\epsilon = 0.4$ and a magnetic shear of $\hat{s} = 0.8$. At the radius $r/a = 0.45$, we take the field line pitch to be $q = 1.39$. The gradient scale lengths are: $R/L_{ni} = R/L_{ne} = 2.2$, and $R/L_{Ti} = R/L_{Te} = 6.9$. The ion temperature is $T_i = T_e = 10$ keV. We use a grid of 32 points along the field line and for velocity space: 16 points in $v$ and 33 points in $\lambda$. When nonlinear simulations are run for this case, a perpendicular box size of $L_x \approx L_y = 63\rho_i$ is used with a resolution of $N_x = N_y = 64$. The main ion species is deuterium, and electrons are assumed adiabatic: $\delta n_e/n_e \equiv \int \delta f_e d^3\mathbf{v}/n_e = e\phi/T_e$. A linearized, conservative collision operator (see Abel et al. 2008; Barnes et al. 2009) was used with $\nu_{ei} = 0.01 v_{ti}/a$.

Unless otherwise stated, the simulations in Secs 3 and 4 have these parameters. The test case of Sec. 5 is described therein.

## 3. The trace-alphas approximation

We inquire: at what concentration do alpha particles begin contributing to the turbulent dynamics? In any of the existing or planned fusion devices, the fraction $n_\alpha/n_e$ is expected to peak at most around 1% (Budny 2002). Considering that alpha particles have such high energy, it is not obvious whether or not they contribute to the electrostatic nonlinear dynamics of the plasma as these densities.

When the density of a charged species is negligible, so is its contribution to the right-hand side of the quasineutrality condition (2.4). In the limit of $n_\alpha \to 0$ (holding $\delta n_\alpha/n_\alpha$ constant), $\phi$ no longer depends on the perturbation $h_\alpha$. In that case the gyrokinetic equation is linear in $h_\alpha$. We can therefore write (2.13) as:

$$\mathscr{L}[h_\alpha, \phi] = -Z_\alpha e \frac{\partial F_{0\alpha}}{\partial E} \frac{\partial \langle \phi \rangle_{\mathbf{R}_s}}{\partial t} - \frac{c}{B}\mathbf{b} \times \nabla \langle \phi \rangle_{\mathbf{R}_s} \cdot \nabla F_{0\alpha}, \tag{3.1}$$

where $\mathscr{L}$ is the linear operator defined by the left-hand side of (2.13), and $\phi$ is treated as a given function of space and time, determined by the turbulent dynamics of the other, non-negligible species. Note that this does not imply that $h_\alpha$ is linear in $\phi$, nor that the usually nonlinear $E \times B$-drift term in (2.13) is ignored. Invert (3.1) to obtain $\delta f_\alpha$ and plug into (2.9). It follows that we can write the particle flux in the form (Angioni and Peeters 2008):

$$\frac{R}{n_\alpha}\Gamma_\alpha = D\frac{R}{L_{n_\alpha}} + D_E \frac{R}{L_{T_e}} + V_p. \tag{3.2}$$

From left to right, the terms are: particle diffusion, thermodiffusion, and the pinch flux (flux at zero gradient). The *electron* temperature gradient appears here because that is the dominant dependence of the $v_c$ parameter when a single ion species is present with $Z_i = 1$ and $n_i \approx n_e$ (see (2.17)).

### 3.1. *Linear theory*

A first estimate of how much of an effect alphas have on the plasma can be obtained by examining the linear growth rate of an unstable ion temperature gradient (ITG) mode. We examine the frequency and growth rate of the $k_y\rho_i = 0.3$ poloidal mode as alpha particles are introduced at ever-increasing density in Fig. 1. The growth rate decreases with increasing alpha particle concentration, but only changes by about 5%

https://doi.org/10.1017/S002237781400124X Published online by Cambridge University Press

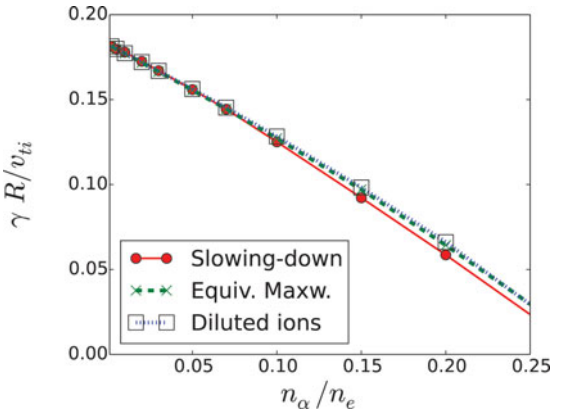



FIGURE 1. Comparison of linear growth rates for different models of alpha particles at a range of concentrations. Calculations were performed by running `GS2` for a single $k_y = 0.3$ mode of the cyclone base case (Dimits et al. 2000) with $R/L_{n\alpha} = R/L_{ni} = R/L_{ne} = 2.2$. Agreement between all three is within 1% up to $n_\alpha/n_e \approx 0.05$, and still within 10% up to an impossibly large $n_\alpha/n_e \approx 0.15$. Note that the equivalent Maxwellian and diluted-ion models are nearly identical.

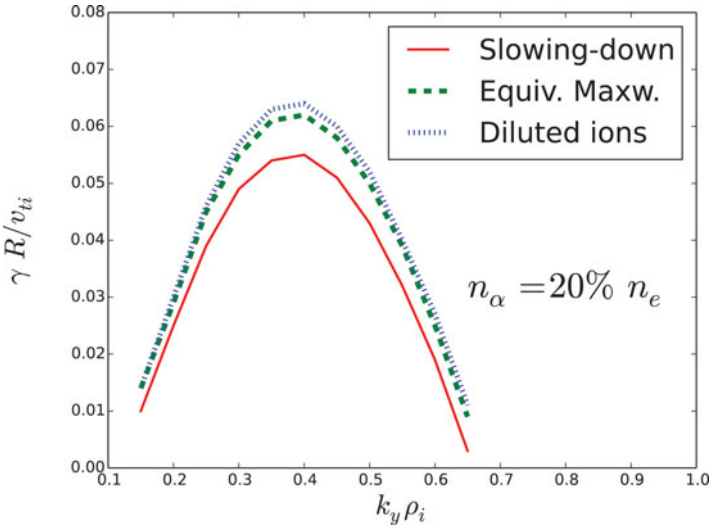



FIGURE 2. Growth rate spectrum of linear ITG growth rate at a 20% alpha particle concentration. Same case as Fig. 1.

up to an alpha particle concentration of 2%. Even at a concentration of 20%, we still see in Fig. 2 that there is no qualitative and little quantitative difference in the poloidal spectrum. We find that the effect of a small population of alpha particles is negligible, at least linearly.

As $n_\alpha/n_e$ increases, the relative fraction of main ions (whose temperature gradient drives the instability) must decrease to compensate and maintain equilibrium quasineutrality, resulting in a dilution effect (see Tardini et al. 2007; Holland et al. 2012). It could be argued whether this effect alone is responsible for the change in growth rate shown in Figs 1 and 2. Therefore, what is also shown (labeled 'diluted ions') is the case where alphas do not contribute to the field at all, even at significant density. Indeed, it takes very high concentrations of alpha particles

https://doi.org/10.1017/S002237781400124X Published online by Cambridge University Press

($\gtrapprox$10%) to distinguish between the different models (see Sec. 4 for an explanation of the 'equivalent Maxwellian' model), and no model at all. This suggests that, even beyond realistic reactor densities, the primary effect of alpha particles is only to dilute the ITG-driving ions, introducing no particularly interesting electrostatic effects of their own.

### 3.2. *Nonlinear simulations*

We then proceed to demonstrate that these conclusions continue to hold in turbulence. We turn on the nonlinear term in (2.13) and examine the evolution of fluxes to an approximate steady-state. The time evolution to saturation of the total heat flux is shown in Fig. 3. In this case, the decrease in outward total heat flux is due to the combined effect of: (1) alpha particles carrying some heat inward; and (2) reducing the ITG drive by the main ions. An inward heat and particle flux for the alpha particles is seen because there is an inward flux of alphas due to the second two terms in (3.2), but the alpha density gradient is not strong enough in this case (with $R/L_{n\alpha} = R/L_{ni}$) for the diffusion term to dominate and drive the alpha particles outward.

Even at high concentrations of alpha particles ($\sim$10%), the effect on the turbulence is indistinguishable from that of mere dilution of the main ions, consistent with linear theory. This is demonstrated in Fig. 5, which shows only a 10% difference between heat fluxes and between the case with alpha particles and that without, wherein the latter of which only the ion dilution effect is taken into account.

To see the effect this has on alpha transport, let us also compare the alpha particle flux. If alphas have little or no effect on the turbulence, we would then expect $\Gamma_\alpha/n_\alpha$ to be constant as the concentration changes. The time-averaged value of $\Gamma_\alpha/n_\alpha$ compared to alpha particle concentration is shown in Fig. 4. It is clear that no significant change occurs below a concentration of about 5%.

As mentioned previously, by assuming energetic ions are of negligible density, it can be shown (see Hauff et al. 2009; Pueschel et al. 2012) that for almost all pitch angles (the dependence on which is not covered in this work since we are focusing on isotropic alpha particles), the diffusion coefficient scales like $E^{-3/2}$. To make sense of this quantity, consider the energy-dependent analog of (3.2) consistent with the energy-dependent flux of (2.6):

$$\frac{R}{F_{0\alpha}(E)}\Gamma_\alpha(E) = D(E)\frac{R}{L_{n_\alpha}} + D_E(E)\frac{R}{L_{T_e}} + V_p(E). \tag{3.3}$$

Note that, with this definition, $D(E)$ has the same units as its energy-integrated counterpart. By performing several nonlinear runs with a range of density gradients, a linear fit of $\Gamma_\alpha(E)$ versus $R/L_{n_\alpha}$ was performed, the slope of which is proportional to the diffusion coefficient $D(E)$. The results are plotted in Fig. 6, with a scaling and approximate magnitude consistent with Hauff et al. (2009) and Pueschel et al. (2012).

The conclusion of this section is to confirm that in the presence of electrostatic turbulence, an energetic species has little effect up to a concentration of at least 2%. However, even beyond such a density, they do not have much of a direct effect on the turbulence. Instead, their effect is simply to dilute the main ions, decreasing the ITG drive. This dilution effect is the dominant influence of fast ions up to at least a concentration of 10%.

https://doi.org/10.1017/S002237781400124X Published online by Cambridge University Press

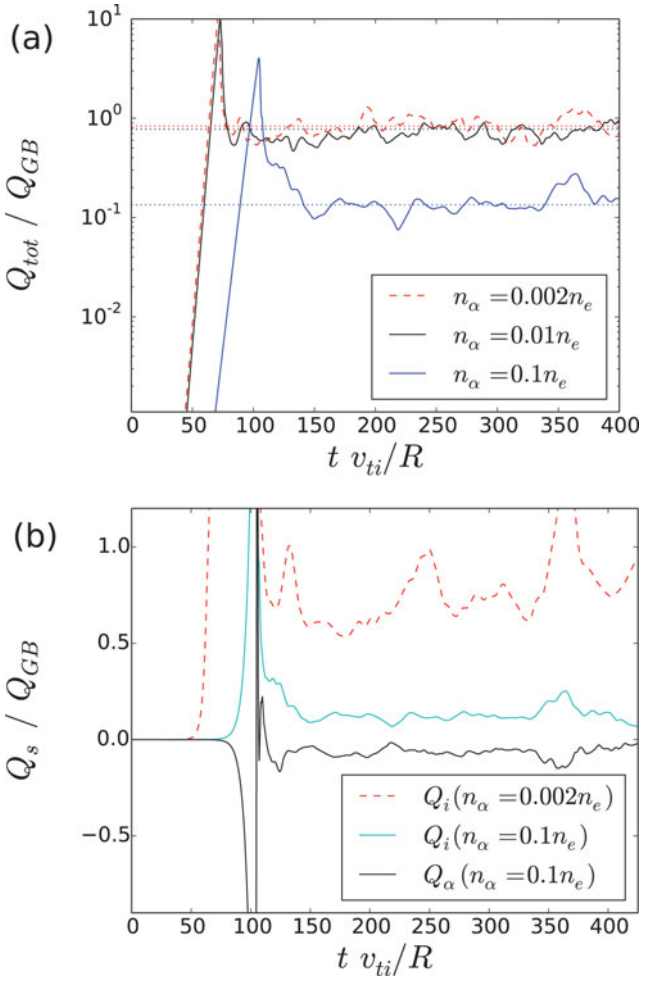



FIGURE 3. Time evolution of the turbulent heat flux. The dotted horizontal lines are the time-averaged heat fluxes for the different concentrations of alpha particles. $Q_{GB} \equiv 2n_e v_{ti} T_i \rho^{*2}$. (*a*) shows the total heat flux for different alpha particle concentrations, and (*b*) shows the breakdown by species at $n_\alpha/n_e = 0.1$, compared to the ion heat flux at negligible alpha density.

## 4. The equivalent-Maxwellian approximation

Even though a concentration of fast ions appears to have little effect on electrostatic turbulence, the response of alpha particles to that turbulence depends quite explicitly on the equilibrium distribution function, and especially its radial gradient.

To take advantage of existing tools to solve the gyrokinetic equation for Maxwellian equilibria, it is naturally suggested that, instead of representing the alpha particles with a slowing-down distribution (e.g. (2.15)), one could instead define a Maxwellian that has the same temperature, and that this may provide satisfactory results. This method of modeling alpha particles has been widely used in gyrokinetic studies of fast ions (see, e.g. Estrada-Mila et al. 2006; Albergante et al. 2009; Angioni et al. 2009; Nishimura 2009; Zhang et al. 2010; Pueschel et al. 2012; Citrin et al. 2013; Mishchenko et al. 2014).

https://doi.org/10.1017/S002237781400124X Published online by Cambridge University Press

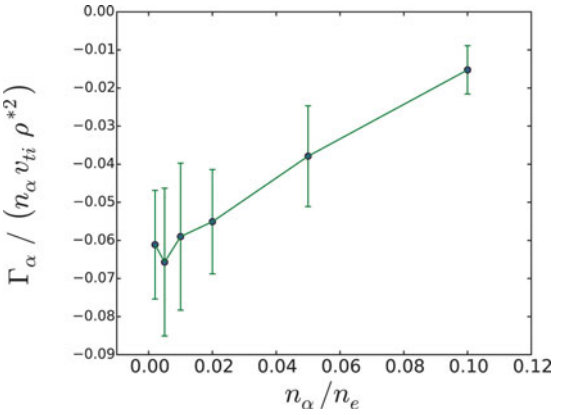



FIGURE 4. Steady-state turbulent flux of alpha particles as a function of alpha particle concentration. Units are gyro-Bohm normalized by the alpha particle density. 'Error bars' indicate the standard deviation of the departure of fluctuations from the time average, and is intended to put into context the variations of flux at low concentration.

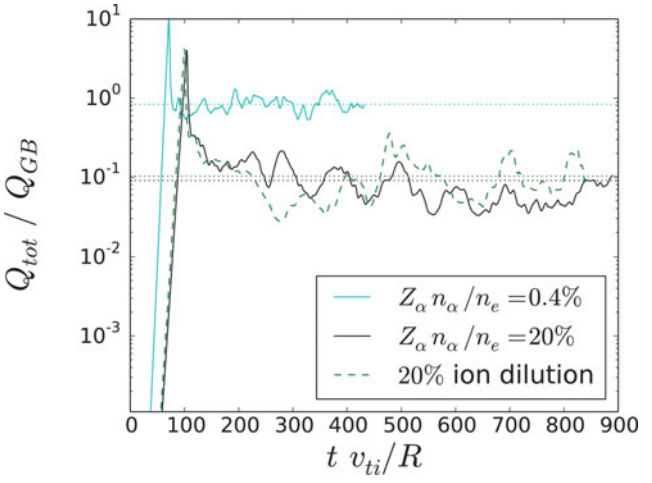



FIGURE 5. Time evolution of the turbulent heat flux, comparing the case of: a small alpha population (solid cyan), a large alpha population (solid black), and a case where the presence of alphas is 'simulated' only be diluting the ion density (dashed green)

### 4.1. *Definitions*

The zeroth and second moment of the slowing-down distribution, (2.15), can be evaluated analytically. We use these to define an effective temperature $T_{\rm eff} = T_{\rm eff}\,(v_c/v_\alpha)$ such that

$$\frac{3}{2} n_\alpha T_{\rm eff} = \int F_{M\alpha} m_\alpha v^2 \, d^3\mathbf{v} = \int F_{S\alpha} m_\alpha v^2 \, d^3\mathbf{v}, \tag{4.1}$$

so (Estrada-Mila et al. 2006)

$$T_{\rm eff} = \frac{m_\alpha v_c^2}{2\ln\left(1 + v_\alpha^3/v_c^3\right)} \times \left[\frac{v_\alpha^2}{v_c^2} - \frac{1}{3}\ln\left(\frac{v_\alpha^2 - v_\alpha v_c + v_c^2}{(v_\alpha + v_c)^2}\right) - \frac{1}{2\sqrt{3}}\tan^{-1}\left(\frac{2v_\alpha - v_c}{\sqrt{3}v_c}\right) - \frac{\pi}{3\sqrt{3}}\right]. \tag{4.2}$$

https://doi.org/10.1017/S002237781400124X Published online by Cambridge University Press

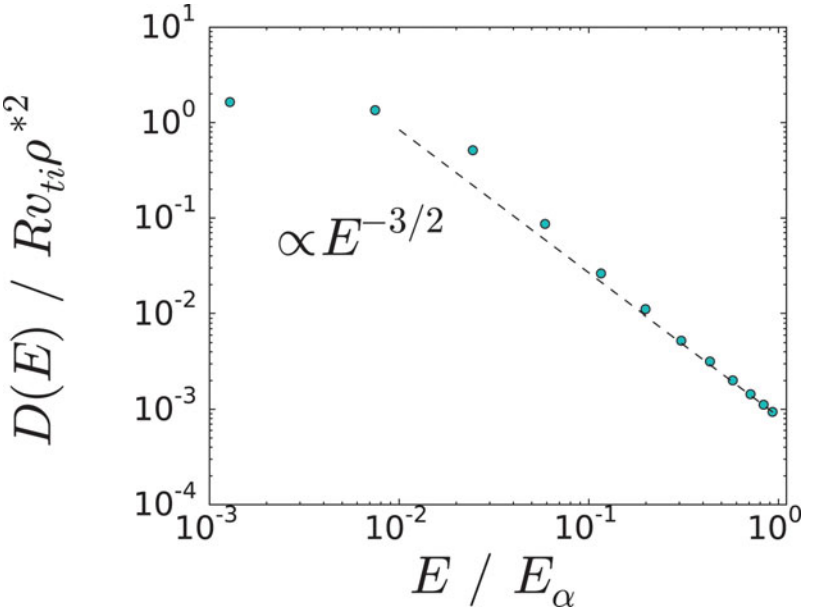



FIGURE 6. Diffusion coefficient of trace alpha particles ($n_\alpha = 0.002 n_e$) as a function of energy.

However, the gradient of the equivalent Maxwellian also appears in the gyrokinetic equation (2.13), so we need a way of calculating it. Fortunately, $v_c$ (hence $T_{\rm eff}$) is a known function of ion and electron parameters, so we can find the effective Maxwellian temperature gradient scale length by using the chain rule, in a manner analogous to (2.17):

$$\frac{\nabla F_{M\alpha}}{F_{M\alpha}} = \frac{\nabla n_\alpha}{n_\alpha} + \frac{1}{T_{\rm eff}}\frac{{\rm d}T_{\rm eff}}{{\rm d}v_c}\left(\frac{\partial v_c}{\partial T_e}\nabla T_e + \frac{\partial v_c}{\partial n_i}\nabla n_i + \frac{\partial v_c}{\partial n_e}\nabla n_e\right)\left(\frac{E}{T_{\rm eff}} - \frac{3}{2}\right). \tag{4.3}$$

We take the derivative of (4.2) and write down an expression for $R/L_{T_{\rm eff}}$ as a function of $x \equiv v_c/v_\alpha$:

$$\frac{R}{L_{T_{\rm eff}}} = \frac{R}{L_{v_c}}\frac{1}{\ln\left(1+x^{-3}\right)}\left[\frac{1}{1+x^3} - \frac{x^2}{3}\left(\frac{E_\alpha}{T_{\rm eff}}\right)\frac{2\pi}{3\sqrt{3}} + \frac{2}{\sqrt{3}}\tan^{-1}\left(\frac{2-x}{\sqrt{3}x}\right)\right.$$
$$\left. + \frac{1}{3}\ln\left(\frac{x^2-x+1}{(1+x)^2}\right) - \frac{x}{(1+x)\left(x^2-x+1\right)}\right] \tag{4.4}$$

where $R/L_{v_c}$ is given by (2.18).

### 4.2. *Linear theory*

Proceeding in a manner analogous to Sec. 3, we analyze the linear mode that results from using a concentration of alpha particles using the equivalent Maxwellian versus the slowing-down distribution. Consistent with Estrada-Mila et al. (2006) (which used a different test case), we find that the growth rates for the slowing-down and Maxwellian distributions in the cyclone base case follow each other very closely up to relatively high concentration (see Fig. 1). This is unsurprising given the conclusion of the previous section: that a modest concentration of alpha particle plays no electrostatic role except dilution.

We proceed to ask the inverse question: how do alpha particles respond to a given linearly unstable eigenfunction, and how does the equilibrium distribution function

https://doi.org/10.1017/S002237781400124X Published online by Cambridge University Press

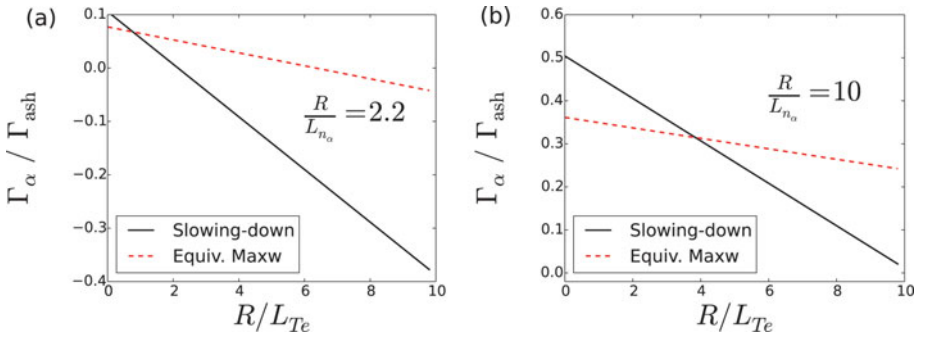



FIGURE 7. Quasilinear alpha particle flux determined by finding linear fits for the coefficients in (3.2). Showing the dependence on the electron temperature gradient for (*a*) $R/L_{n_\alpha} = R/L_{n_i} = 2.2$, and (*b*) $R/L_{n_\alpha} = 10$.

used affect the result? We can use quasilinear theory to estimate the fluxes with the same method as Angioni and Peeters (2008). That is, for each set of parameters, we choose a single unstable mode and calculate the alpha particle flux (2.9) as a function of time. Because it is exponentially growing, we must normalize it to a quantity growing at the same rate, such as the flux of ash (a helium species at the same temperature as the ions). This only works because in both cases, the density is taken to be trace, otherwise there would be a small but catastrophic difference in growth rates. This ratio of alpha flux to ash flux in response to the linear eigenfunction is what we calculate.

Consider again the fact that, in the trace limit, the gyrokinetic equation is linear in the gradients. Then, (3.2) holds, and the particle flux is easily found after finding the coefficients $D$, $D_E$, and $V_p$. After fitting these coefficients to a series of linear simulations for the cyclone case, we plot the dependence of particle flux on the dominant parameters ($R/L_{n_\alpha}$ and $R/L_{T_e}$) in Fig. 7. From inspection, one can see that, depending on the problem parameters, one can achieve anything from very good to very poor agreement between the slowing-down distribution and the equivalent Maxwellian.

### 4.3. *Explanation of discrepancy*

To explain this disagreement, consider the $\nabla F_{0\alpha}$ term in the gyrokinetic equation (2.13). For a Maxwellian distribution, $\nabla F_{M\alpha}/F_{M\alpha}$ is linear in energy (see (4.3)), but the gradient of the slowing-down distribution has a different energy dependence (see (2.17)). From Fig. 8, we see that when $E \sim T_i$ (near which the interaction with the ion-scale turbulence is expected to be the strongest), the gradient of $F_{0\alpha}$ is off by over an order of magnitude. This stark difference in the right-hand side of (2.13) ultimately carries through to the particle flux, resulting in the discrepancies in Figs 7 and 9(b).

We conclude that the equivalent Maxwellian approximation is wrong precisely because it fails to capture the energy dependence of $\nabla F_{0\alpha}$, and at least sometimes strongly disagrees at the most relevant energies. In the diffusive limit, where the gradient of $F_{0\alpha}$ is dominated by $\nabla n_\alpha$, this energy dependence is not important, and one would expect the equivalent Maxwellian to predict at least the correct order of magnitude. Even so, if one wishes to find the gradient $R/L_{n\alpha}$ that eliminates the alpha particle flux, the balance with $D_E$ (which *is* sensitive to the energy dependence of $\nabla F_{S\alpha}$) and $V_p$ in (3.2) and (3.3) is necessary.

### 4.4. *Nonlinear simulations*

One can see in Fig. 7(a) that the 'fully mixed' cyclone base case ($R/L_{n_\alpha} = 2.2$, $R/L_{T_e} = 6.9$) is a particularly poorly performing case for the equivalent Maxwellian.

https://doi.org/10.1017/S002237781400124X Published online by Cambridge University Press

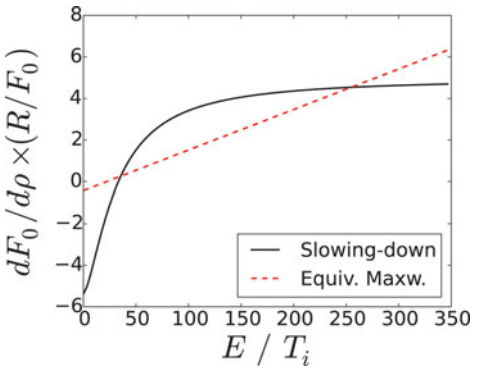



FIGURE 8. Comparing the energy dependence of the radial spatial derivative of $F_{0\alpha}$ for the two models of alpha particle distributions. In both cases, the gradient is found from the density gradient of alpha particles, and the gradient of $v_c$, which can be found as a function of the equilibrium parameters of other species, particularly $T_e$.

Using these parameters, Fig. 9(a) compares the total heat flux for the two distributions. Since they are both well below the threshold to be considered 'trace', there is little statistical difference in the total heat flux between these two, as would be expected. However, the turbulent fluxes shown in Fig. 9(b) demonstrate that the equivalent Maxwellian gets the wrong direction of the alpha particle flux and is off by more than an order of magnitude.

While we do not claim that this strong of a disagreement will be seen in all relevant cases, the observation that: (a) such an agreement is so sensitive to the parameters of the problem; (b) a drastic difference is found for such a common test case as cyclone; and (c) that such an agreement, when it does exist by coincidence, has no physical basis, should be enough to convince the reader that any results for alpha particle flux obtained by using an equivalent-Maxwellian ought to be treated with skepticism. Any disagreement in the fluxes is especially troublesome if one is performing a critical-gradient analysis to determine the alpha particle profile. From inspection of Fig. 7, one can observe very different critical gradients (the gradient for which $\Gamma_\alpha \to 0$) between the two distribution functions.

### 4.5. *Correcting the equivalent Maxwellian*

We can take advantage of the trace approximation to decompose the energy dependence of the transport coefficients given in (3.3). Doing so will allow one to obtain the fluxes that one would get from a simulation with the slowing-down distribution, provided the coefficients $D$, $D_E$ and $V_p$ are known from a series of equivalent Maxwellian simulations.

Consider again the linearity of (3.1). Decompose the right-hand side into terms with the known velocity dependencies of $\partial F_0/\partial E$ and $\nabla F_0$ factored out. When using the slowing-down distribution, we can write the gyrokinetic equation as:

$$\frac{1}{F_{S\alpha}}\mathscr{L}\left[h_\alpha\right] = a_0 M_0^{(S)} + a_1 M_1^{(S)}\frac{R}{L_{n_\alpha}} + a_2 M_2^{(S)}\frac{R}{L_{v_c}}. \tag{4.5}$$

Analogously for the equivalent Maxwellian:

$$\frac{1}{F_{M\alpha}}\mathscr{L}\left[h_\alpha\right] = a_0 M_0^{(M)} + a_1 M_1^{(M)}\frac{R}{L_{n_\alpha}} + a_2 M_2^{(M)}\frac{R}{L_{v_c}}. \tag{4.6}$$

https://doi.org/10.1017/S002237781400124X Published online by Cambridge University Press

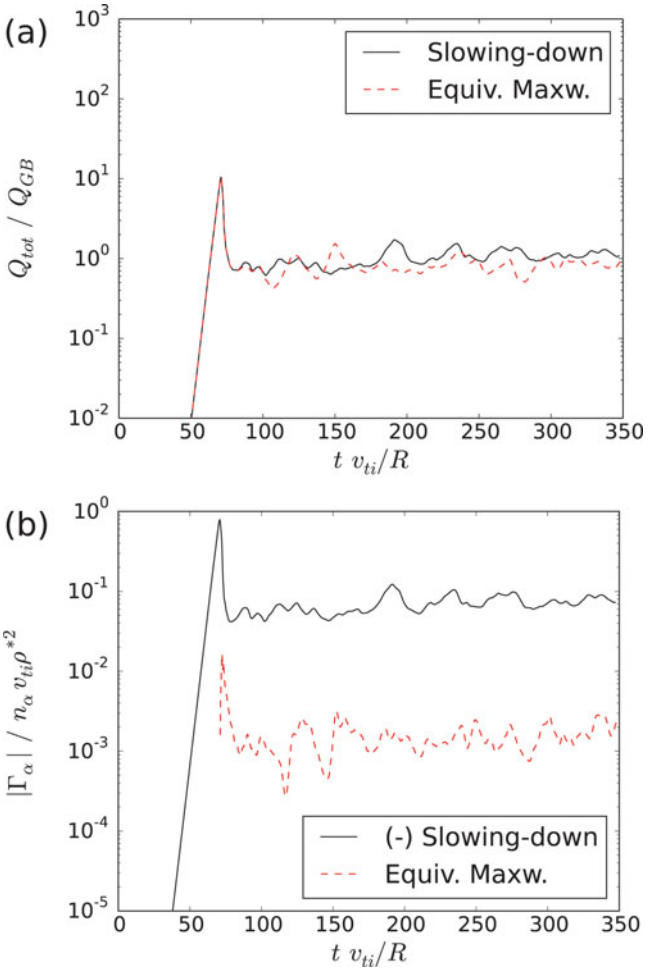



FIGURE 9. Time evolution of (a) total heat flux, and (b) alpha particle flux. Comparing two models for the alphas particles: the slowing-down distribution (solid black), and the equivalent Maxwellian (dashed red). In both cases, the alpha particle concentration is 0.1%. The negative particle flux for the slowing-down distribution is shown, since the signs do not agree.

The following quantities are defined:

$$M_0^{(S)} = -E_\alpha \frac{\partial}{\partial E} \ln F_{S\alpha} = \frac{3}{2}\frac{v^2 v_\alpha}{v_c^3 + v^3} \tag{4.7}$$

$$M_0^{(M)} = -E_\alpha \frac{\partial}{\partial E} \ln F_{M\alpha} = \frac{E_\alpha}{T_{\text{eff}}} \tag{4.8}$$

$$M_1^{(S)} = M_1^{(M)} = 1 \tag{4.9}$$

$$M_2^{(S)} = v_c \frac{\partial}{\partial v_c} \ln F_{S\alpha} = \frac{3v_\alpha^3}{v_c^3 + v_\alpha^3} \frac{1}{\ln\left(1 + v_\alpha^3/v_c^3\right)} - \frac{3v_c^3}{v_c^3 + v^3} \tag{4.10}$$

$$M_2^{(M)} = v_c \frac{\partial T_{\text{eff}}}{\partial v_c} \frac{\partial}{\partial T_{\text{eff}}} \ln F_{M\alpha} = \left(\frac{E}{T_{\text{eff}}} - \frac{3}{2}\right) \frac{L_{v_c}}{L_{T_{\text{eff}}}}, \tag{4.11}$$

where $L_{v_c}$ and $L_{T_{\text{eff}}}$ are given by (2.18) and (4.4) respectively. These factors together contain the only dependence on $F_0$ that appear in the gyrokinetic equation. The

https://doi.org/10.1017/S002237781400124X Published online by Cambridge University Press

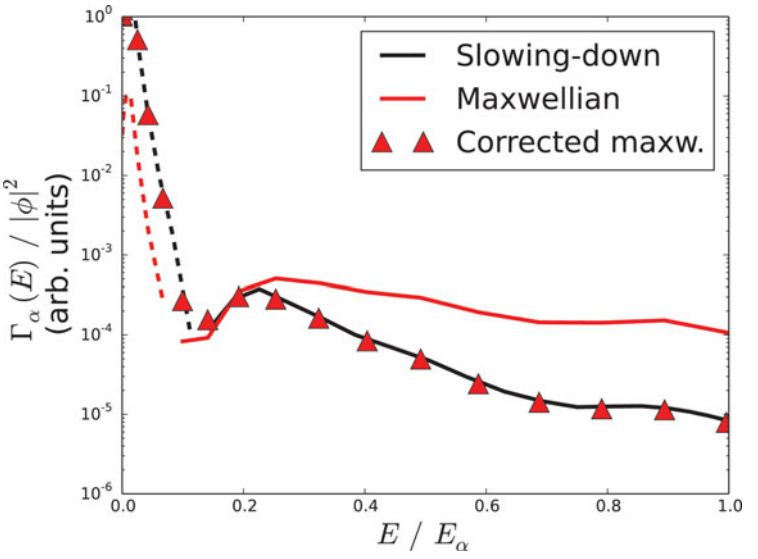



FIGURE 10. Quasilinear radial flux for the $k_y\rho_i = 0.3$ mode normalized to the total amplitude of $\phi$. Triangles represent adjustments made directly to the equivalent Maxwellian via (4.12)–(4.14). Dashed lines represent negative values.

other factors $a_0$, $a_1$, and $a_2$ are allowed to depend on velocity, but not through $F_0$. Therefore, these factors are the same in both (4.5) and (4.6), and the dependence on the equilibrium distribution is entirely contained in the *a priori*-known functions $M_0$, $M_1$, and $M_2$.

Suppose we know, from a simulation campaign using the equivalent Maxwellian approximation, the energy-dependent diffusion coefficients $D^{(M)}(E)$, $D_E^{(M)}(E)$, and $V_p^{(M)}(E)$. We can find the corresponding turbulent transport coefficients $D^{(S)}(E)$, $D_E^{(S)}(E)$, $V_p^{(S)}(E)$, and hence the radial flux $\Gamma_\alpha(E)$ for the slowing-down distribution, even if a gyrokinetic simulation with $F_{S\alpha}$ was never run. To convert between the two:

$$D^{(S)}(E) = D^{(M)}(E) \tag{4.12}$$

$$D_E^{(S)}(E) = \frac{M_2^{(S)}}{M_2^{(M)}} D_E^{(M)}(E) \tag{4.13}$$

$$V_p^{(S)}(E) = \frac{M_0^{(S)}}{M_0^{(M)}} V_p^{(M)}(E), \tag{4.14}$$

and apply (3.3). For the case whose nonlinear particle flux is shown in Fig. 9, these relationships were applied to the quasilinear flux of the fastest-growing mode. Figure 10 shows the $\Gamma_\alpha(E)$ that results when the equivalent Maxwellian is corrected.

Note that the energy-dependent diffusion coefficient is identical between the two distributions. This is by construction in the way we have defined it in (3.3) (following Angioni and Peeters (2008); Hauff et al. (2009) and Pueschel et al. (2012)). This also explains why there is better agreement in $\Gamma_\alpha(E)$ at higher gradients: the diffusion term tends to dominate. However, to obtain a reasonable estimate for the integrated particle flux in this regime, one must normalize properly by $F_{S\alpha}$. Again, we caution against taking this diffusive approximation too far, for example, in performing a critical gradient analysis, where the other terms in (3.3) do indeed become important.

https://doi.org/10.1017/S002237781400124X Published online by Cambridge University Press

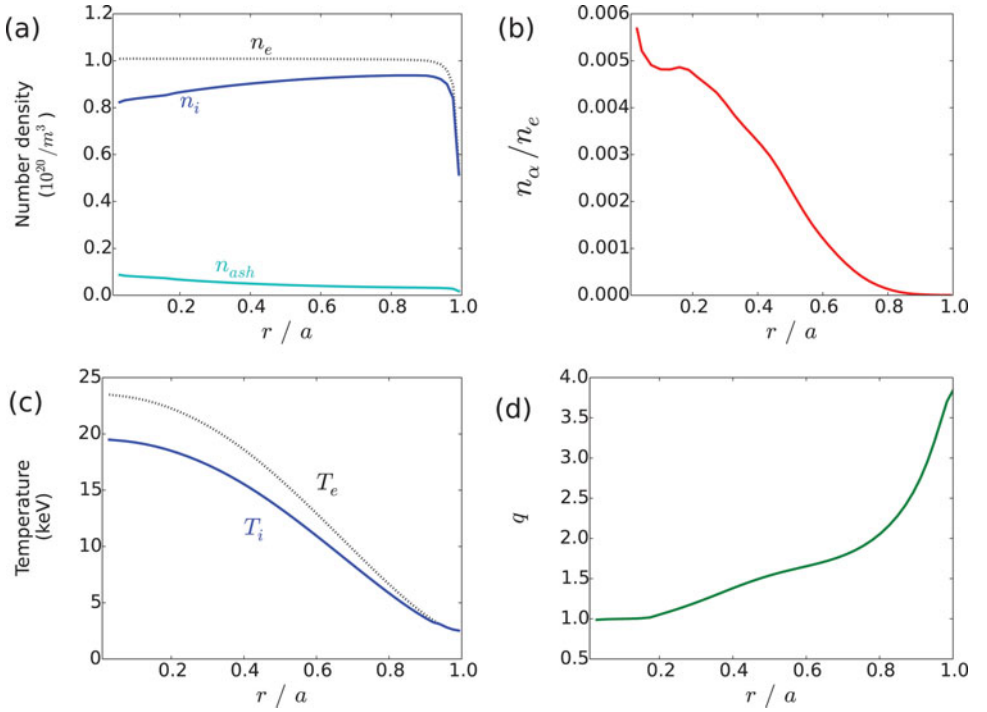



FIGURE 11. Global steady-state profiles for ITER shot 10010100. For these plots, $r$ is the half-diameter on the plane of the magnetic axis, and serves to label the flux surface. Plots show, as a function of radius, (a) number density of bulk ions, electrons and cold He ash, (b) relative concentration of alpha particles, (c) temperature, and (d) safety factor $q$

However, the use of the conversions (4.12)–(4.14) should be adequate even for this purpose so long as alpha particles remain trace.

## 5. Confinement of alpha particles in ITG turbulence

Implicit in the use of the slowing-down distribution (2.15) is the assumption that alpha particles are well confined in the sense that all collisional slowing-down happens on approximately the same flux surface: that the particle transport time is long compared to the slowing-down time. In this section, we will analyze this assumption and its associated subsidiary expansion introduced in Sec. 2 using the results from a nonlinear local ITER simulation. Said analysis will be *a posteriori*: assuming a classical slowing-down velocity distribution for fast alpha particles, how likely is it that it remains so when taking into account turbulent transport?

### 5.1. *Test case*

We choose to depart from the cyclone base case since it is based on the geometry of DIII-D, a tokamak for which the flux tube approximation is questionable for alpha particles. The test case here is a projected ITER ELMy H-mode scenario (case #10010100) from the CCFE 2008 public release database (Campbell 2001; Budny 2002; Roach et al. 2008), and the radial profiles were simulated with the `PTRANSP` code. Figure 11 shows radial profiles of some of the equilibrium properties. We will use a Miller expansion of the geometry about a flux tube on the surface defined by $r/a = 0.6$, which gives the following geometrical properties: safety factor $q = 1.66$,

https://doi.org/10.1017/S002237781400124X Published online by Cambridge University Press

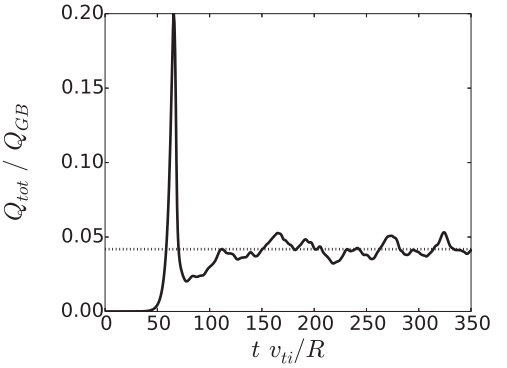



FIGURE 12. The time-evolution of the total heat flux for the ELMy H-mode ITER shot 10010100.

magnetic shear $\hat{s} = 0.39$, ellipticity $\kappa = 1.53$ (with $a\kappa'(r) = 0.35$), triangularity $\delta = 0.22$ ($a\delta'(r) = 0.41$), and a Shafronov shift derivative of $\Delta'(r) = -0.097$. Electrons were assumed to be adiabatic again, with an alpha particle concentration of $n_\alpha/n_e = 0.12\%$, and an ash concentration of $n_{\rm ash}/n_e = 7.9\%$. The gradient length scales were $a/L_{n_e} = 0.0$, $a/L_{n_i} = -0.37$, $a/L_{n_{\rm ash}} = 0.95$, $a/L_{n_\alpha} = 6.9$, and $a/L_{T_i} = a/L_{T_e} = a/L_{T_{\rm ash}} = 2.2$. The main ions were taken to be a species with an averaged mass weighted by the density of deuterium, tritium, and a small amount of heavy impurities, resulting in $m_i/m_D = 1.484$, and $Z_i = 1$. The ash is assumed to be at the same temperature as the ions: $T_i = 0.847T_e$, and $T_e = 10.9$ keV. The box size is $318.9\rho_i \times 157\rho_i$ in $x$ and $y$ respectively, with $N_x = 144$ and $N_y = 96$. This large box size is not strictly necessary, but is to ensure that many alpha-particle gyroradii fit inside the simulation domain. The parallel and velocity-space resolutions were the same as for cyclone above: $N_\theta = 32$, $N_v = 16$, and $N_\lambda = 33$. The total heat flux resulting from this simulation is show in Fig. 12 for reference.

### 5.2. *Characteristic time scales*

Define the alpha particle transport time as a characteristic timescale on which the turbulent particle flux acts. It is found by balancing the appropriate terms in the transport equation:

$$\frac{\partial F_{0\alpha}}{\partial t} + \nabla \cdot \boldsymbol{\Gamma}(E) \sim \frac{F_{0\alpha}}{\tau_\Gamma} - \frac{\Gamma(E)}{L_{n_\alpha}}, \tag{5.1}$$

where $L_{n_\alpha}$ is chosen as the characteristic length scale on which the alpha particle flux varies. This serves to define:

$$\tau_\Gamma(E) \equiv \frac{L_{n_\alpha} F_{0\alpha}}{\Gamma(E)}. \tag{5.2}$$

We wish to compare this transport time to a timescale representative of the effects of collisions. The energy-diffusion term is given by:

$$C_E\left[F_{0\alpha}\right] = \sum_{s=i,e} \frac{1}{v^2}\frac{\partial}{\partial v}\left(\nu_s^{\alpha s} v^3 F_{0\alpha} + \frac{1}{2}\nu_\parallel^{\alpha s} v^4 \frac{\partial F_{0\alpha}}{\partial v}\right), \tag{5.3}$$

where:

$$\nu_s^{\alpha s} = \frac{16\pi n_s Z_s^2 e^4 \ln \Lambda_{\alpha s}}{m_\alpha}\frac{1}{T_s}\frac{v_\alpha}{v} G\left(\frac{v}{v_{ts}}\right), \tag{5.4}$$

https://doi.org/10.1017/S002237781400124X Published online by Cambridge University Press

$$\nu_{\parallel}^{\alpha s} = \frac{16\pi n_s Z_s^2 e^4 \ln \Lambda_{\alpha s}}{m_\alpha^2} \frac{2}{v^3} G\left(\frac{v}{v_{ts}}\right), \tag{5.5}$$

and $G$ is the Chandrasekhar function:

$$G(x) \equiv \frac{\mathrm{Erf}(x) - \frac{2x}{\sqrt{\pi}} e^{-x^2}}{2x^2}. \tag{5.6}$$

In the limit $v_{ti} \ll v \ll v_{te}$, the collision operator is dominated by the $\nu_s^{\alpha e}$ term, and at lower energies, $\nu_s^{\alpha i}$ and $\nu_{\parallel}^{\alpha i}$ become more important. For the slowing-down distribution $\partial F_{S\alpha}/\partial v = -3v^2 F_{S\alpha}/\left(v_c^3 + v^3\right)$, so we will use this to estimate the derivative in the $\nu_{\parallel}$ terms in (5.3) for a slightly more general $F_{0\alpha}$.

Adding all these terms, we can define a total collision time by:

$$\frac{1}{\tau_c} \sim \frac{1}{F_{0\alpha}} C_E\left[F_{0\alpha}\right] \approx \sum_{s=i,e} \frac{16\pi n_s Z_s^2 e^4 \ln \Lambda_{\alpha s}}{m_\alpha^2} \left[\frac{m_\alpha}{T_s v} - \frac{3}{v_c^3 + v^3}\right] G\left(\frac{v}{v_{ts}}\right). \tag{5.7}$$

Now, by comparing (5.2) and (5.7), we can make a reasonable estimate of how relevant a transport term would be in an equation like (2.5). This is shown in Fig. 13. Around $E_\alpha = 3.5$ MeV, we see that collisions are dominant over transport, and $\tau_c$ flattens out to the slowing-down time $\tau_s$ as expected. Also, if $\tau_\Gamma$ is interpreted as a particle confinement time, we expect hot alphas to be well confined on the order of several seconds. This is roughly consistent with previous work (see Angioni et al. 2009). Our local estimate for the actual alpha particle confinement time (defined as the average number of alpha particles leaving a flux surface divided by the total number of particles contained within the flux surface) is about 2.4 s in our simulation, roughly consistent with the energy confinement time estimated in Table 1.

However, at lower energies, but still well above the ion or ash temperatures, the radial transport of alpha particles becomes important compared to collisions. For this case, it can be seen in Fig. 13(b) that the relative importance peaks near the critical speed, but there is no reason to believe that this is more than coincidence: there are a number of parameters that could, in principle, be independently tuned. For example, the transport time scale scales quadratically with both $\rho^*$ and $L_{n\alpha}$, neither of which would have a direct effect on the characteristic collision time.

Note that these simulations were run with adiabatic electrons; kinetic electrons would change the numerical value of the flux and thus the ratio of collision time to transport time. However, in our experience, including kinetic electrons generally tends to increase the fluctuation amplitudes, which would increase the alpha particle flux accordingly. Therefore, the analysis presented here is a best-case scenario: more rigorous simulations with kinetic electrons would make any modification to the slowing-down distribution even stronger.

## 6. Summary and discussion

In this work, we have laid out our framework for employing gyrokinetics to study the behavior of isotropic non-Maxwellian fast ions. From first principles, we critically analyze several common assumptions made in the analysis of hot alpha particles. The basic conclusion is that, electrostatically, alpha particles react only passively to ion-scale turbulence. Even at high charge densities of around 20% of the total charge, it is clear from the rough magnitude of the flux that the effect is simply that of diluting the drive from bulk ions.

https://doi.org/10.1017/S002237781400124X Published online by Cambridge University Press

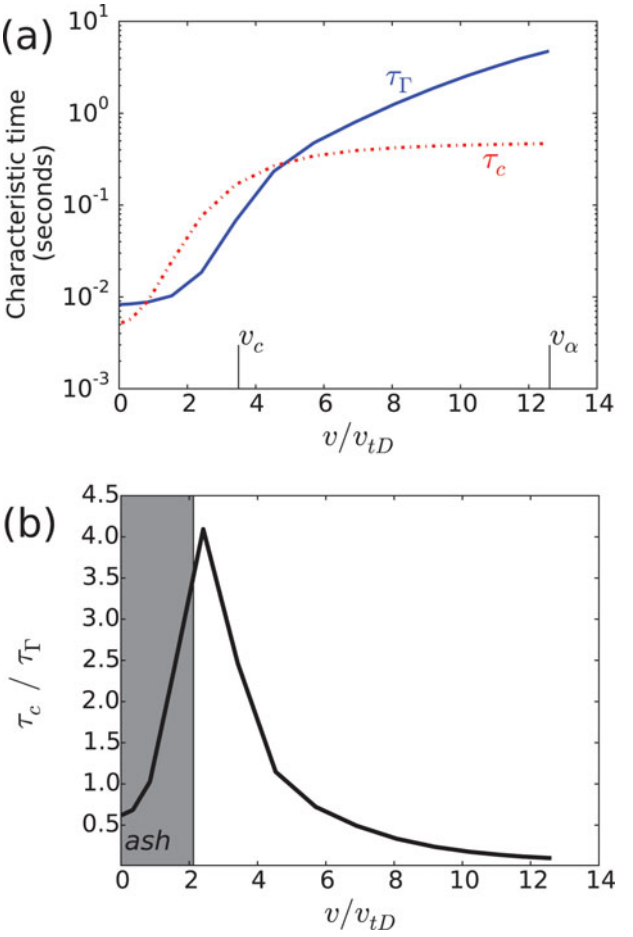



FIGURE 13. Comparing characteristic transport time ($\tau_\Gamma$) and collision time ($\tau_c$) as a function of velocity. (a) shows the characteristic times directly, whereas (b) shows the relative importance of radial transport compared to collisions: $\tau_c/\tau_\Gamma$. The shaded region represents the area up to $v = 3 \times v_{t,\mathrm{ash}}$ (assuming $T_{\mathrm{ash}} = T_i$), where the slowing-down distribution is not valid and is dominated by Maxwellianized helium ash. The critical speed $v_c$ and birth speed $v_\alpha$ have been marked for reference.

On the other hand, if one wishes to analyze in what manner are the alpha particles are advected by the background turbulence, it is clear even from the order-of-magnitude results presented here and from linear theory that the correct distribution function must be used. The reason for this is because the perturbed distribution function depends linearly on the radial gradient of the equilibrium distribution. If an incorrect model distribution is used (e.g. the 'equivalent Maxwellian'), applying the correct velocity-space dependence of $\nabla F_{S\alpha}$ either presupposes the relevant region of velocity space (e.g. by employing a linear fit to Fig. 8 near $E = 0$), or is not based on physical principles. At least three major gyrokinetic codes (`GS2`, `GENE` (Dannert et al. 2008), and `GYRO` (Waltz and Bass 2014)) have the capability to model non-Maxwellian species, so there is little reason to continue using an inadequate model. Previous effort spent by other groups in the analysis of alpha particles using the equivalent Maxwellian is certainly not wasted, however. As long as alpha particles

https://doi.org/10.1017/S002237781400124X Published online by Cambridge University Press

are trace, a direct analytic conversion between the two is possible and was presented in (4.12)–(4.14).

Armed with a good analytical estimate of the equilibrium distribution at high energy: the classical slowing-down distribution, we proceed to analyze the strength of advection relative to collisionality as a function of energy. Where the ratio of these characteristic scales approaches or exceeds unity, the slowing-down distribution itself is expected to be wrong. Our analysis of a projected ITER shot shows that this is indeed the case. This means that, although alpha particles are predicted to be well confined overall (consistent with experiment, see Pace et al. (2013)), energy-dependent transport is strong enough to affect the slow time evolution of the equilibrium distribution function, at least at some energies for some combination of reasonable parameters. The very high-energy part of the slowing-down tail near 3.5 MeV remains relatively unaffected by the turbulence, as expected.

It should be kept in mind that ours is a local flux-tube analysis. Depending on the tokamak, shot, and radius, the gradient length scales can change significantly over the orbit size of a high-energy alpha particle. By restricting ourselves to ITER shots or significantly uniform profiles, we strive to alleviate this concern. Another caveat is that our analysis has ignored the parallel nonlinearity, which ought to be included for a weakly-collisional species. It is believed that the primary results presented herein are robust to these caveats, but additional study of these effects is of course welcome.

Our results clearly suggest that a transport study capturing the coupled radial and energy dependence of the alpha particle distribution is warranted. By using a passive tracer model with transport coefficients found from a series of fully nonlinear simulations, one can evolve $F_{0\alpha}(v, r)$. It is this distribution which ought to be used locally to obtain more confident results for the behavior of alpha particles.

## Acknowledgements

The authors would like to thank M. Barnes, F. Parra, G. Hammett, and A. Schekochihin for their ideas and insightful discussions, G. Colyer for the use of computer time on Helios, and T. Fredian for his help in accessing the CCFE public tokamak profile database. The Wolfgang Pauli Institute in Vienna and CIEMAT in Madrid have graciously hosted workshops and meetings at which much of this work was inspired and performed. The use of the Helios (IFERC) and Edison (NERSC) supercomputers have been critical to the results presented here. This material is based upon work supported by the U.S. Department of Energy, Office of Science, Office of Fusion Energy Science, under award numbers DEFG0293ER54197 and DEFC0208ER54964.

## REFERENCES

Abel, I., Barnes, M., Cowley, S. C., Dorland, W. and Schekochihin, A. 2008 Linearized model Fokker-Planck collision operators for gyrokinetic simulations. I. Theory. *Phys. Plasmas* **15**, 122 509.

Abel, I., Plunk, G. G., Wang, E., Barnes, M., Cowley, S. C., Dorland, W. and Schekochihin, A. A. 2013 Multiscale gyrokinetics for rotating tokamak plasmas: fluctuations, transport and energy flows. *Rep. Prog. Phys.* **76**, 116 201.

Abel, I. and Schekochihin, A. In preparation.

Albergante, M., Graves, J. P., Fasoli, A., Jenko, F. and Dannert, T. 2009 Anomalous transport of energetic particles in ITER relevant scenarios. *Phys. Plasmas* **16**, 112 301.

https://doi.org/10.1017/S002237781400124X Published online by Cambridge University Press

Angioni, C. and Peeters, A. G. 2008 Gyrokinetic calculations of diffusive and convective transport of $\alpha$ particles with a slowing-down distribution function. *Phys. Plasmas* **15**, 052 307.

Angioni, C., Peeters, A. G., Pereverzev, G. V., Bottino, A., Candy, J., Dux, R., Fable, E., Hein, T. and Waltz, R. E. 2009 Gyrokinetic simulations of impurity, He ash and $\alpha$ particle transport and consequences on ITER transport. *Nucl. Fusion* **49**, 055 013.

Barnes, M., Abel, I., Dorland, W., Ernst, D. R., Hammett, G. W., Ricci, Paolo, Rogers, B. N., Schekochihin, A. and Tatsuno, T. 2009 Linearized model Fokker-Planck collision operators for gyrokinetic simulations. II. Numerical implementation and tests. *Phys. Plasmas* **16**, 072 107.

Brizard, A. and Hahm, T. S. 2007 Foundations of nonlinear gyrokinetic theory. *Rev. Mod. Phys.* **79**, 421.

Budny, R. 2002 Fusion alpha parameters in tokamaks with high DT fusion rates. *Nucl. Fusion* **42**, 1383.

Campbell, D. J. 2001 The physics of the international thermonuclear experimental reactor FEAT. *Phys. Plasmas* **8**, 2041.

Candy, J., Holland, C., Waltz, R. E., Fahey, M. R. and Belli, E. 2009 Tokamak profile prediction using direct gyrokinetic and neoclassical simulation. *Phys. Plasmas* **16**, 060 704.

Candy, J. and Waltz, R. E. 2003 An Eulerian gyrokinetic-Maxwell solver. *J. Comput. Phys.* **186**, 545.

Citrin, J. et al. 2013 Nonlinear stabilization of tokamak microturbulence by fast ions. *Phys. Rev. Lett.* **111**, 155 001.

Cowley, S. C., Kulsrud, R. M. and Sudan, R. 1991 Considerations of ion-temperature-gradient-driven turbulence. *Phys. Fluids B Plasma Phys.* **3**, 2767.

Dannert, T., Gunter, S., Hauff, T., Jenko, F., Lapillonne, X. and Lauber, P. 2008 Turbulent transport of beam ions. *Phys. Plasmas* **15**, 062 508.

Dimits, A. M. et al. 2000 Comparisons and physics basis of tokamak transport models and turbulence simulations. *Phys. Plasmas* **7**, 969.

Dorland, W., Jenko, F., Kotschenreuther, M. and Rogers, B. N. 2000 Electron temperature gradient turbulence. *Phys. Rev. Lett.* **85**, 5579.

Estrada-Mila, C., Candy, J. and Waltz, R. E. 2006 Turbulent transport of alpha particles in reactor plasmas. *Phys. Plasmas* **13**, 112 303.

Frieman, E. A. and Chen, L. 1982 Nonlinear gyrokinetic equations for low-frequency electromagnetic waves in general plasma equilibria. *Phys. Fluids* **25**, 502.

Gaffey, J. D. 1976 Energetic ion distribution resulting from neutral beam injection in tokamaks. *J. Plasma Phys.* **16**, 149.

Hauff, T., Pueschel, M. J., Dannert, T. and Jenko, F. 2009 Electrostatic and magnetic transport of energetic ions in turbulent plasmas. *Phys. Rev. Lett.* **102**, 075 004.

Helander, P. and Sigmar, D. 2002 *Collisional Transport in Magnetized Plasmas*. Cambridge University Press, Cambridge.

Holland, C., Petty, C. C., Schmitz, L., Burrell, K. H., McKee, G. R., Rhodes, T. L. and Candy, J. 2012 Progress in GYRO validation studies of DIII-D H-mode plasmas. *Nucl. Fusion* **52**, 114 007.

Jenko, F., Dorland, W., Kotschenreuther, M. and Rogers, B. N. 2000 Electron temperature gradient driven turbulence. *Phys. Plasmas* **7**, 1904.

Kotschenreuther, M., Rewoldt, G. and Tang, W. M. 1995 Comparison of initial value and eigenvalue codes for kinetic toroidal plasma instabilities. *Comput. Phys. Commun.* **88**, 128.

Li, B. and Ernst, D. R. 2011 Gyrokinetic Fokker-Planck collision operator. *Phys. Rev. Lett.* **106**, 195 002.

Mishchenko, A., Könies, A. and Hatzky, R. 2014 Gyrokinetic particle-in-cell simulations of Alfvén eigenmodes in presence of continuum effects. *Phys. Plasmas* **21**, 052 114.

Nave, M. F. F. et al. and Contributors to the JET-EFDA Workprogramme 2003 Role of sawtooth in avoiding impurity accumulation and maintaining good confinement in JET radiative mantle discharges. *Nucl. Fusion* **43**, 1204.

Nishimura, Y. 2009 Excitation of low-n toroidicity induced Alfven eigenmodes by energetic particles in global gyrokinetic tokamak plasmas. *Phys. Plasmas* **16**, 030 702.

Pace, D. C. et al. 2013 Energetic ion transport by microturbulence is insignificant in tokamaks. *Phys. Plasmas* **20**, 056 108.

https://doi.org/10.1017/S002237781400124X Published online by Cambridge University Press

Pueschel, M. J., Jenko, F., Schneller, M., Hauff, T., Gunter, S. and Tardini, G. 2012 Anomalous diffusion of energetic particles: connecting experiment and simulations. *Nucl. Fusion* **52**, 103 018.

Roach, C.et al. 2008 The 2008 public release of the international multi-tokamak confinement profile database. *Nucl. Fusion* **48**, 125 001.

Rosenbluth, M. N. and Rutherford, P. H. 1975 Excitation of alfven waves by high-energy ions in a tokamak. *Phys. Rev. Lett.* **34**, 1428.

Stix, T. 1973 Heating of toroidal plasmas by neutral injection. *Plasma Physics* **14**, 367.

Sugama, H. and Horton, W. 1998 Nonlinear electromagnetic gyrokinetic equation for plasmas with large mean flows. *Phys. Plasmas* **5**, 2560.

Tardini, G. et al. 2007 Thermal ions dilution and ITG suppression in ASDEX Upgrade ion ITBs. *Nucl. Fusion* **47**, 280.

Waltz, R. E. and Bass, E. M. 2014 Prediction of the fusion alpha density profile in ITER from local marginal stability to Alfvén eigenmodes. *Nucl. Fusion* **54**, 104 006.

Zhang, W., Decyk, V., Holod, I., Xiao, Y., Lin, Z. and Chen, L. 2010 Scalings of energetic particle transport by ion temperature gradient microturbulence. *Phys. Plasmas* **17**, 055 902.

https://doi.org/10.1017/S002237781400124X Published online by Cambridge University Press